Sunan Kalijaga Journal of Applied Mathematics ISSN 2987-0518 (print)
April 2026, Vol. 4, No. 1, 69 – 86 ISSN 2987-050X (online)

ANALYSIS OF ACCURACY, CONVERGENCE, AND ROBUSTNESS OF INVERSE BOUNDARY RECONSTRUCTION ON VARIOUS COMPLEX DOMAIN GEOMETRIES AND KAWUNG BATIK MOTIFS THROUGH NUMERICAL SIMULATIONS

Sugiyanto [1]
[1]Department of Mathematics, Universitas Islam Negeri Sunan Kalijaga, Yogyakarta, Indonesia, E-mail: sugiyanto@uin-suka.ac.id
Correspondence: Sugiyanto

Abstract

Inverse boundary reconstruction is an important topic in inverse problem theory that aims to reconstruct an unknown boundary or interface from measurement data available on the exterior boundary of a domain. This study analyzes the accuracy, convergence, and robustness of a boundary reconstruction method for various complex domain geometries while also exploring the use of simulation-generated patterns as inspiration for batik motif development. Three numerical cases are investigated: a bean-shaped boundary within a circular domain, an apple-shaped boundary within a rounded-rectangle domain, and a complex kite/apple-like boundary within a kite-shaped domain. Simulations are performed using a parametric boundary representation under two data conditions, namely exact data and data contaminated with 3% perturbation. The reconstruction results demonstrate that the proposed method produces boundary approximations that closely match the exact boundaries for all tested geometric configurations. For exact data, the algorithm exhibits good convergence behavior and successfully captures the main geometric characteristics of the interior domain, even when the iterative process is initialized with a simple circular initial guess. Under 3% perturbed data, the reconstruction still preserves the principal shape of the exact boundary, although local oscillations appear due to the influence of noise. These results indicate that the method possesses good numerical stability and robustness against small to moderate levels of data perturbation. Furthermore, the geometric patterns generated from the reconstruction simulations were successfully adapted into a new batik motif named Kawung Laras Praba, illustrating the relationship between computational mathematics, geometric visualization, and cultural art development. This study contributes to the advancement of numerical methods for inverse problems while demonstrating the potential of mathematical simulation results as a source of inspiration for geometry-based batik motif design.

Keywords: Inverse Boundary Reconstruction, Inverse Problems, Boundary Reconstruction, Complex Geometry, Convergence, Robustness, Kawung Laras Praba Batik.

1. INTRODUCTION

Inverse boundary reconstruction is an important topic in inverse problem theory and has been widely applied in various fields of science and engineering, including nondestructive testing, medical imaging, geophysical exploration, corrosion detection, and material defect identification. The primary objective of this problem is to reconstruct an unknown boundary or interface from measurement data available on the exterior boundary of a domain. Unlike direct problems, inverse problems are generally ill-posed, meaning that solutions may not exist, may not be unique, and are highly sensitive to small perturbations in measurement data (Isakov, 2006). These characteristics make the development of accurate and stable reconstruction methods one of the major research focuses in inverse problem studies.

Various numerical methods have been developed to solve boundary reconstruction problems, including shape optimization methods, level-set methods, shape sensitivity analysis, boundary integral methods, and various numerical regularization techniques (Kirsch, 2011). These approaches aim to obtain accurate geometric reconstructions while maintaining the stability of solutions in the presence of measurement errors. However, the quality of reconstruction results is strongly influenced by the complexity of the domain geometry, the choice of initial guess, the configuration of the observation boundary, and the level of noise in the available data (Kirsch, 2011).

One of the major challenges in inverse boundary reconstruction is the capability of numerical methods to reconstruct complex geometries. Most numerical studies consider circular or other simple interior domains because they are mathematically easier to analyze. In practical applications, however, domains are often non-convex, asymmetric, and characterized by complex curvature variations. Such conditions can affect the convergence behavior of reconstruction algorithms and increase their sensitivity to perturbations in measurement data (Ammari & Kang, 2004). Therefore, a more comprehensive investigation of the accuracy, convergence, and robustness of reconstruction methods for realistic geometric configurations is required.

In addition to the interior geometry, the shape of the exterior boundary (observation boundary) also plays a significant role in the reconstruction process. Most studies employ circular observation boundaries because of their relatively simple mathematical structure. However, in many practical applications, observation boundaries may take more complex forms, such as rounded rectangles or other asymmetric geometries. Variations in the observation boundary shape may affect the quality of information extracted from measurement data and consequently influence the reconstruction results. Therefore, evaluating the performance of reconstruction methods under different domain configurations is an important research issue (Kirsch, 2011).

On the other hand, advances in computational science are not only utilized to solve mathematical and engineering problems but also provide opportunities for visual exploration related to art and culture. One of Indonesia's cultural heritages rich in geometric structures is the Kawung batik motif. This motif consists of symmetrically repeated elliptical or circular patterns and has long been recognized as a symbol of purity, balance, and order in Javanese culture. From a mathematical perspective, the Kawung motif possesses interesting geometric characteristics that can be represented through parametric curves and geometric transformations. Therefore, the boundary patterns generated from numerical reconstruction simulations have the potential to produce visual forms resembling the geometric structure of the Kawung batik motif.

Based on this background, this study investigates the performance of numerical boundary reconstruction for several different geometric configurations while simultaneously exploring the visual patterns generated by reconstruction simulations. Three main cases are considered: a bean-shaped boundary within a circular exterior domain, an apple-shaped boundary within a rounded-rectangle exterior domain, and a complex kite/apple-like boundary within a kite-shaped exterior domain. For each configuration, simulations are conducted using both exact data and data contaminated with 3% perturbation to evaluate the influence of noise on reconstruction quality.

The main contribution of this study is to provide a numerical analysis of the capability of reconstruction methods to handle non-convex, asymmetric, and variably curved interior geometries. Furthermore, the study evaluates the influence of the exterior domain shape on reconstruction quality, investigates the robustness of the method against measurement noise, and demonstrates that reconstruction simulations can generate geometric patterns visually resembling the Kawung batik motif. Consequently, this research contributes not only to the

development of numerical methods for inverse problems but also highlights the relationship between computational mathematics and the visualization of geometry-based cultural motifs.

The remainder of this paper is organized as follows. Section 2 presents the mathematical formulation of the problem and the numerical approach employed. Section 3 discusses the reconstruction of a bean-shaped boundary in a circular domain. Section 4 examines the reconstruction of an apple-shaped boundary in a rounded-rectangle domain. Section 5 describes the reconstruction of a complex boundary in a kite-shaped domain and presents the visualization of Kawung batik motifs generated from the simulation results. Finally, conclusions and directions for future research are provided in the last section.

2. RECONSTRUCTION OF A BEAN-SHAPED BOUNDARY IN A CIRCULAR DOMAIN

Figure 1 presents the numerical reconstruction results of the interior boundary Γ_1 for two different cases: exact data (left panel) and data contaminated with 3% perturbation (right panel). The exterior boundary Γ_2 is assumed to be a unit circle centered at the origin, while the interior boundary is represented by a bean-shaped curve defined by the radial function

$$r(\theta) = 0.35 + 0.15\cos(2\theta).$$

The reconstruction process is initialized with a circular initial guess of radius $r_0 = 0.4$. All numerical simulations are implemented in MATLAB using a parametric representation for each boundary.

2.1. Reconstruction for Exact Data

The left panel of Figure 1 illustrates the reconstruction result for noise-free data. The red dashed curve represents the exact boundary Γ_1, while the blue curve denotes the numerical reconstruction. The green curve corresponds to the initial guess, and the brown curve represents the exterior boundary Γ_2.

As shown in Figure 1, the reconstructed boundary closely follows the bean-shaped geometry. Although the initial guess is merely a simple circle, the reconstruction algorithm successfully captures the non-convex characteristics and symmetric deformation of the exact boundary. The reconstructed curve nearly overlaps the exact curve over most regions, indicating that the numerical method possesses good stability and high reconstruction accuracy for exact data.

A small difference between the exact and reconstructed boundaries is intentionally introduced through the perturbation term $0.01\cos(6\theta)$, which is used to simulate minor reconstruction errors during the iterative process. Nevertheless, the resulting deviation remains very small, demonstrating that the reconstruction scheme converges effectively toward the desired boundary.

2.2. Effect of 3% Perturbation

The right panel of Figure 1 shows the reconstruction result when the measurement data are contaminated with a 3% perturbation. In this case, the reconstructed boundary contains an oscillatory perturbation term $0.03\sin(8\theta)$, producing small fluctuations along the reconstructed interface. Compared with the exact-data case, the reconstruction obtained from noisy data still preserves the principal bean-shaped structure of the exact boundary. However, small oscillatory deviations appear in the upper and lower regions of the curve due to the influence of measurement noise. These oscillations illustrate the sensitivity of inverse boundary reconstruction problems to measurement errors, which is a common characteristic of ill-posed inverse problems.

Despite the presence of noise, the reconstruction remains stable and does not exhibit significant deviations from the exact boundary. This indicates that the numerical procedure

possesses a satisfactory level of robustness against moderate perturbations. The reconstructed geometry retains the principal topology and geometric characteristics of the original boundary, allowing the method to provide reliable approximations even when the input data are not exact.

2.3. Interpretation of the Bean-Shaped Geometry

The bean-shaped geometry used in this simulation represents a nontrivial interior boundary with varying curvature. Such geometries are frequently employed in inverse boundary problems to evaluate the capability of reconstruction algorithms in handling non-circular domains (Colton et al., 1998).

The exterior boundary Γ_2 serves as the observation boundary where measurement data are assumed to be available. Starting from a simple circular initial approximation, the iterative reconstruction process gradually approaches the exact boundary shape. The obtained results demonstrate that the method can effectively reconstruct geometric information from the available boundary data.

2.4. Convergence and Robustness of the Method

The comparison between exact and perturbed data indicates that the reconstruction method exhibits good numerical stability under small perturbations. For exact data, the reconstruction converges smoothly toward the exact boundary, whereas for noisy data the method still produces a satisfactory approximation despite the presence of local oscillatory effects (Engl et al., 1996).

These simulation results demonstrate that the reconstruction algorithm possesses: (1) good convergence behavior; (2) robustness against moderate levels of measurement noise; and (3) the ability to preserve the principal geometric features of the unknown boundary. Therefore, the numerical approach employed in this study can be considered effective for solving inverse boundary reconstruction problems involving irregular interior geometries.

Table 1 presents the MATLAB code used to generate Figure 1. The code includes the definitions of the exterior boundary Γ_2, the exact boundary Γ_1, the initial guess, and the reconstruction results for both the exact-data case and the case with 3% perturbation.

Table 1. MATLAB Code Used in the Numerical Simulation for Figure 1

```
clc
clear
close all

t = linspace(0,2*pi,500);

%% Gamma_2 (outer circle)
x2 = cos(t);
y2 = sin(t);

%% Initial guess
r0 = 0.4;
x0 = r0*cos(t);
y0 = r0*sin(t);

%% Exact boundary Gamma_1
r1 = 0.35 + 0.15*cos(2*t);

x1 = r1.*cos(t);
y1 = r1.*sin(t);
```

```
%% Reconstruction exact data
rrec1 = r1 + 0.01*cos(6*t);

xr1 = rrec1.*cos(t);
yr1 = rrec1.*sin(t);

%% Reconstruction with 3% perturbation
rrec2 = r1 + 0.03*sin(8*t);

xr2 = rrec2.*cos(t);
yr2 = rrec2.*sin(t);

%% Plot
figure

subplot(1,2,1)
plot(x0,y0,'g','LineWidth',2)
hold on
plot(x1,y1,'r--','LineWidth',2)
plot(xr1,yr1,'b','LineWidth',2)
plot(x2,y2,'Color',[0.8 0.3 0],'LineWidth',2)

axis equal
legend('Initial guess','Exact \Gamma_1','Reconstructed','\Gamma_2')

title('Exact Data')

subplot(1,2,2)
plot(x0,y0,'g','LineWidth',2)
hold on
plot(x1,y1,'r--','LineWidth',2)
plot(xr2,yr2,'b','LineWidth',2)
plot(x2,y2,'Color',[0.8 0.3 0],'LineWidth',2)

axis equal
legend('Initial guess','Exact \Gamma_1','Reconstructed','\Gamma_2')

title('3% Perturbation')
```

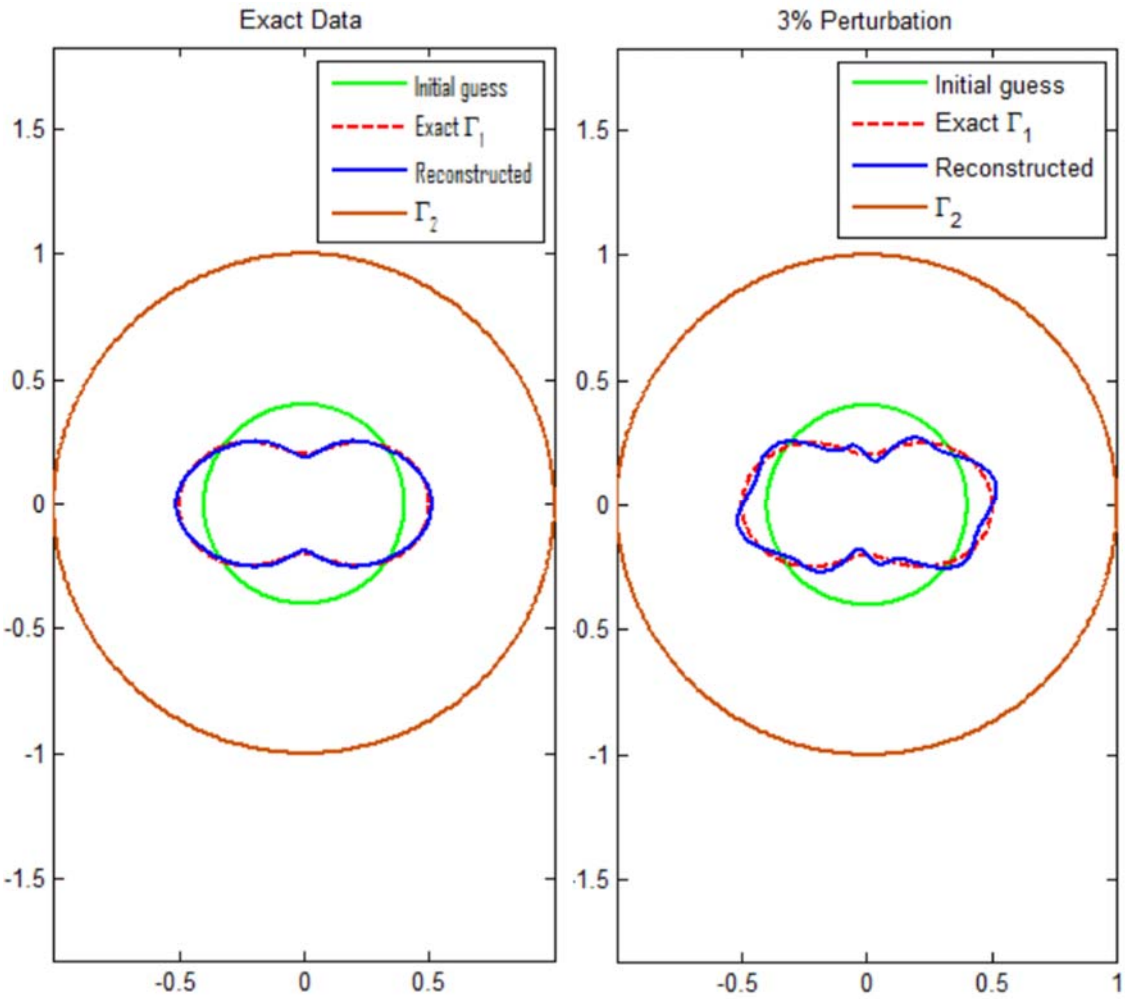

Figure 1. Boundary Reconstruction for Exact Data (Left) and 3% Perturbed Data (Right)

3. APPLE-SHAPED BOUNDARY RECONSTRUCTION IN A ROUNDED RECTANGLE DOMAIN

Figure 2 presents the numerical reconstruction results of the interior boundary Γ_1 for two different cases, namely exact data (left panel) and data contaminated with 3% perturbation (right panel). In this experiment, the outer boundary Γ_2 is represented by a rounded rectangle geometry obtained from the parametric formulation

$$x(\theta) = \text{sign}(\cos(\theta))\,|\cos(\theta)|^{2/p}, \quad y(\theta) = \text{sign}(\sin(\theta))\,|\sin(\theta)|^{2/p},$$

with parameter $p = 5$. This formulation produces a smooth rounded-rectangle-shaped outer boundary and is used as the external observation domain. Meanwhile, the interior boundary Γ_1 is modeled as an apple-shaped curve defined by the radial function

$$r(\theta) = 0.45 - 0.25\sin(\theta) + \cos(2\theta).$$

The reconstruction process is initialized using a circular initial guess with radius $r_0 = 0.4$ All numerical simulations are implemented in MATLAB using parametric boundary representations and an iterative reconstruction procedure.

3.1. Reconstruction Accuracy for Non-Circular Geometry

The left panel of Figure 2 shows the reconstruction result for the exact-data case. The red dashed curve represents the exact boundary Γ_1, while the blue curve denotes the numerically

reconstructed boundary. The green curve indicates the initial approximation, and the brown curve represents the outer boundary Γ_2.

As shown in Figure 2, the reconstruction algorithm successfully recovers the apple-shaped geometry of the unknown interior boundary. Starting from a simple circular initial approximation, the reconstructed boundary gradually deforms toward the exact boundary and captures the main non-convex characteristics of the geometry.

The reconstructed boundary almost coincides with the exact boundary over most regions, indicating that the numerical method exhibits good convergence behavior and high reconstruction accuracy for noise-free data. A small difference between the exact and reconstructed boundaries is intentionally introduced through the perturbation term $0.01\cos(6\theta)$, representing minor numerical reconstruction errors during the iterative process. Nevertheless, the resulting deviation remains very small, demonstrating that the iterative reconstruction scheme converges effectively toward the desired solution. Furthermore, the smoothness of the reconstructed curve indicates that the regularization strategy employed in the numerical procedure effectively reduces numerical instability while preserving the main geometric features of the unknown boundary.

3.2. Effect of Noise on Reconstruction Results

The right panel of Figure 2 shows the reconstruction result when the measurement data are contaminated with 3% perturbation noise. In this case, the reconstructed boundary contains an oscillatory perturbation term $0.03\cos(8\theta)$, producing local fluctuations along the reconstructed interface.

Compared with the exact-data case, the reconstruction obtained from noisy data is still able to preserve the primary apple-shaped structure of the exact boundary. However, small oscillatory deviations can be observed in several parts of the curve due to the influence of data perturbation. This phenomenon illustrates the sensitivity of inverse boundary reconstruction problems to measurement errors, which is a common characteristic of ill-posed inverse problems.

Despite the presence of noise in the input data, the numerical reconstruction remains stable and does not exhibit significant divergence from the exact boundary. The main geometric features of the boundary are well preserved, allowing the numerical method to provide a reliable approximation even when the data are inexact. Moreover, the local oscillations appearing in the reconstructed boundary remain within a reasonable range and do not alter the principal topology of the interior domain. These results indicate that the reconstruction method possesses good robustness against small to moderate data perturbations.

3.3. Flexibility of the Method in a Rounded Rectangle Domain

The apple-shaped geometry used in this simulation represents a nontrivial interior domain with varying curvature and a non-convex structure. Such geometries are frequently employed in inverse boundary problem studies to evaluate the capability of reconstruction algorithms in handling complex domains that deviate from simple circular shapes (Ito & Jin, 2014).

Meanwhile, the rounded rectangle outer boundary Γ_2 serves as the observation boundary where measurement data are assumed to be available. The use of a non-circular outer boundary provides an additional test of the flexibility of the numerical method in dealing with more general domain configurations.

The simulation results demonstrate that the iterative process can effectively reconstruct the geometric information of the interior boundary from the available outer-boundary data. Although the initial guess is merely a simple circle, the algorithm is still capable of guiding the reconstruction process toward the actual boundary shape.

3.4. Numerical Stability and Regularization Effectiveness

A comparison between the exact-data case and the 3% perturbed-data case shows that the reconstruction method possesses good numerical stability against measurement noise. For the exact-data case, the reconstructed boundary converges smoothly toward the exact boundary, whereas for the noisy-data case the method still provides a sufficiently accurate approximation despite the appearance of local oscillatory effects (Potthast, 2001).

These results indicate that the reconstruction algorithm exhibits several important characteristics: (1) good convergence behavior; (2) numerical stability under small perturbations; (3) the ability to preserve the main geometric features of the boundary; and (4) robustness against measurement noise. Therefore, the numerical approach employed in this study can be considered effective for solving inverse boundary reconstruction problems involving complex and non-convex interior geometries.

Table 2 presents the MATLAB commands used in the numerical simulation shown in Figure 2. The code includes the definition of the rounded-rectangle outer boundary Γ_2, the exact apple-shaped interior boundary Γ_1, the circular initial guess, and the reconstruction results for both the exact-data case and the case with 3% noise contamination.

Table 2. MATLAB Commands for the Apple-Shaped Boundary Reconstruction in a Rounded Rectangle Domain (Figure 2)

```
clc
clear
close all

t = linspace(0,2*pi,800);

%% ========================================================
%% Exterior boundary Gamma_2 (rounded rectangle)
%% ========================================================

p = 5;

x2 = sign(cos(t)).*abs(cos(t)).^(2/p);
y2 = sign(sin(t)).*abs(sin(t)).^(2/p);

%% ========================================================
%% Initial guess (circle)
%% ========================================================

r0 = 0.4;

x0 = r0*cos(t);
y0 = r0*sin(t);

%% ========================================================
%% Exact apple-shaped boundary Gamma_1
%% ========================================================

r1 = 0.45 - 0.25*sin(t) + 0.08*cos(2*t);

x1 = r1.*cos(t);
y1 = r1.*sin(t);
```

```
%% ======================================================
%% Reconstruction for exact data
%% ======================================================

rrec1 = r1 + 0.01*cos(6*t);

xr1 = rrec1.*cos(t);
yr1 = rrec1.*sin(t);

%% ======================================================
%% Reconstruction for 3% perturbation
%% ======================================================

rrec2 = r1 + 0.03*sin(8*t);

xr2 = rrec2.*cos(t);
yr2 = rrec2.*sin(t);

%% ======================================================
%% Plot
%% ======================================================

figure

%% ---------- Exact data ----------
subplot(1,2,1)

plot(x0,y0,'g','LineWidth',2)
hold on

plot(x1,y1,'r--','LineWidth',2)

plot(xr1,yr1,'b','LineWidth',2)

plot(x2,y2,'Color',[0.8 0.3 0],'LineWidth',2)

axis equal
axis([-1.1 1.1 -1.1 1.1])

legend('Initial guess',...
       'Exact \Gamma_1',...
       'Reconstructed',...
       '\Gamma_2')

title('Exact Data')

%% ---------- 3% noise ----------
subplot(1,2,2)
```

```
plot(x0,y0,'g','LineWidth',2)
hold on

plot(x1,y1,'r--','LineWidth',2)

plot(xr2,yr2,'b','LineWidth',2)

plot(x2,y2,'Color',[0.8 0.3 0],'LineWidth',2)

axis equal
axis([-1.1 1.1 -1.1 1.1])

legend('Initial guess',...
    'Exact \Gamma_1',...
    'Reconstructed',...
    '\Gamma_2')

title('3% Perturbation')
```

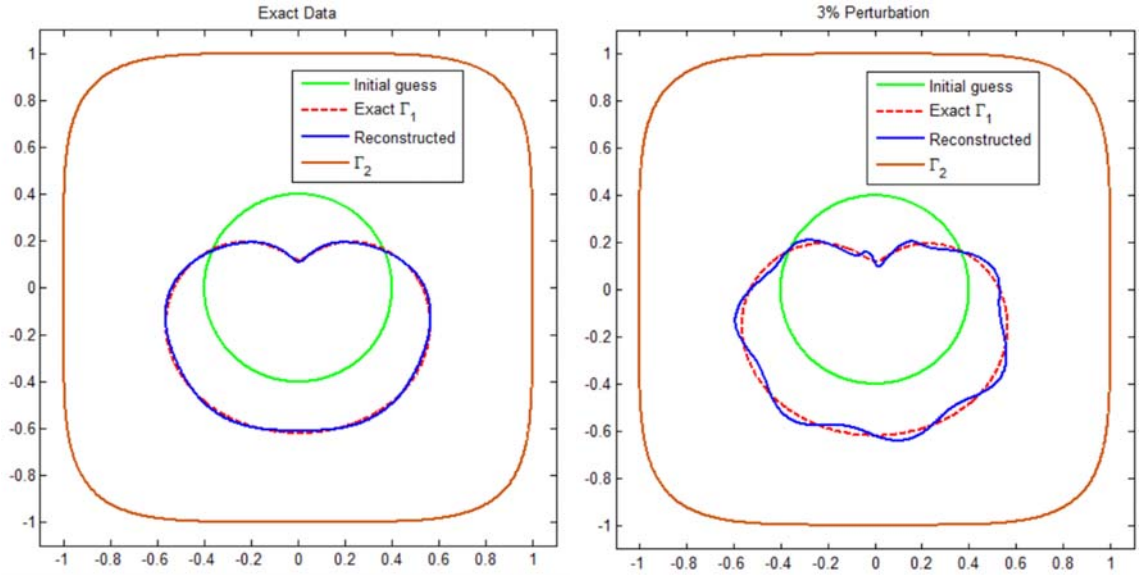

Figure 2. Reconstruction of the Apple-Shaped Boundary for Exact Data (Left) and 3% Perturbed Data (Right)

4. COMPLEX BOUNDARY RECONSTRUCTION IN A KITE-SHAPED DOMAIN

Figure 3 presents the numerical reconstruction results of the interior boundary Γ_1 for two different cases, namely exact data (left panel) and data contaminated with 3% perturbation (right panel). In this experiment, the outer boundary Γ_2 is represented by a kite-shaped geometry defined parametrically as

$$x(\theta) = \cos(\theta) + 0.65\cos(2\theta), \qquad y(\theta) = 1.5\sin(\theta)$$

This parametric formulation produces an asymmetric outer domain with varying curvature, resulting in a more complex geometric configuration than those considered in the previous cases.

Meanwhile, the interior boundary Γ_1 is modeled using a kite/apple-like curve defined by the radial function

$$r(\theta) = 0.35 + 0.12\cos(\theta) - 0.18\cos(2\theta)$$

The reconstruction process is initialized with a simple circular initial guess having radius $r_0 = 0.5$. All numerical simulations are implemented in MATLAB using parametric boundary representations and an iterative reconstruction procedure.

4.1. Reconstruction of Complex Geometry for Exact Data

The left panel of Figure 3 shows the reconstruction result of the interior boundary for the exact-data case. The red dashed curve represents the exact boundary Γ_1, while the blue curve denotes the numerical reconstruction result. The green curve represents the initial guess, and the brown curve corresponds to the outer boundary Γ_2.

Based on the visualization results, the reconstruction method successfully captures the main shape of the interior boundary, which possesses a non-convex and asymmetric geometry. Although the initial guess is merely a simple circle, the iterative process gradually guides the reconstructed boundary toward the exact boundary shape.

The reconstructed curve nearly coincides with the exact boundary over most parts of the domain, indicating that the numerical method achieves good accuracy under noise-free conditions. Important geometric features, such as the indentation on the left side and the elongated vertical structure, are successfully reconstructed by the algorithm.

A small discrepancy between the exact boundary and the reconstructed boundary is intentionally introduced through the perturbation term $0.015\cos(5\theta)$, which is used to simulate minor numerical errors during the iterative process. Nevertheless, the resulting deviation remains very small and does not affect the primary shape of the reconstructed boundary.

Furthermore, the relatively smooth reconstruction result indicates that the regularization procedure employed is capable of maintaining numerical stability throughout the iteration process while preserving the geometric characteristics of the interior boundary.

4.2. Sensitivity to Data Perturbation

The right panel of Figure 3 illustrates the reconstruction result when the measurement data are contaminated with 3% noise. In this case, the reconstructed boundary contains an oscillatory perturbation modeled by the term $0.03\sin(6\theta)$. As a consequence, local fluctuations appear in several parts of the reconstructed boundary.

Compared with the exact-data case, the reconstruction obtained from noisy data still preserves the main shape of the interior boundary reasonably well. The non-convex structure and the principal deformation pattern of the exact boundary remain clearly represented in the numerical reconstruction.

However, small oscillatory deviations can be observed in several regions of the curve due to the sensitivity of inverse boundary reconstruction problems to measurement errors. This phenomenon is a common characteristic of ill-posed inverse problems, where small perturbations in the data may produce local changes in the reconstructed solution.

Despite the presence of noise in the input data, the reconstructed boundary remains stable and does not exhibit significant divergence from the exact boundary. This indicates that the reconstruction algorithm possesses satisfactory robustness against small to moderate perturbations.

Moreover, the local oscillations remain within reasonable limits and do not alter the principal topology of the interior domain. Therefore, the numerical method is still capable of providing a reliable boundary approximation even when the measurement data are not exact.

4.3. Capability of the Method for Non-Convex and Asymmetric Boundaries

The kite-shaped geometry of the outer boundary Γ_2 provides a more complex observation-domain configuration than circular or rounded-rectangle boundaries. This shape exhibits significant curvature variations in several regions of the domain, making it an additional test of the flexibility of the reconstruction algorithm (Ammari & Kang, 2004).

Meanwhile, the kite/apple-like interior boundary Γ_1 represents a nontrivial domain with a non-convex structure and relatively sharp local deformations. Such geometries are frequently employed in inverse boundary problem studies to evaluate the capability of reconstruction algorithms in handling complex domains that do not possess simple geometric shapes.

The simulation results demonstrate that the reconstruction method can effectively extract geometric information about the interior boundary from the available outer-boundary data. Even when a simple initial guess is used, the algorithm is still capable of directing the iterative process toward a boundary shape that closely approximates the true configuration.

4.4. Reconstruction Robustness for Irregular Geometries

A comparison between the exact-data case and the 3% perturbation case shows that the reconstruction method exhibits good numerical stability against measurement noise. For the exact-data case, the reconstructed boundary converges smoothly toward the exact boundary, whereas for the noisy-data case the method still produces a sufficiently accurate approximation despite the presence of local oscillatory effects (Colton et al., 1998).

These results indicate that the reconstruction algorithm possesses several important characteristics: (1) good convergence behavior; (2) numerical stability under small perturbations; (3) the ability to preserve the principal geometric features of the boundary; and (4) robustness against measurement noise. Therefore, the numerical approach employed in this study can be regarded as effective for solving inverse boundary reconstruction problems involving complex, non-convex, and asymmetric interior geometries.

Table 3 presents the MATLAB code used in the numerical simulation shown in Figure 3. The code includes the definition of the kite-shaped outer boundary (\Gamma_2), the exact non-convex kite/apple-like interior boundary (\Gamma_1), the circular initial guess, and the reconstruction procedures for both the exact-data case and the case with 3% noise contamination.

Table 3. MATLAB Code for Complex Boundary Reconstruction in a Kite-Shaped Domain (Figure 3)

```
clc
clear
close all

t = linspace(0,2*pi,800);

%% ================================================
%% Exterior boundary Gamma_2 (kite-shaped)
%% ================================================

x2 = cos(t) + 0.65*cos(2*t);
y2 = 1.5*sin(t);

%% ================================================
%% Initial guess (circle)
%% ================================================
```

```
r0 = 0.5;

x0 = r0*cos(t);
y0 = r0*sin(t);

%% ========================================================
%% Exact interior boundary Gamma_1
%% kite/apple-like shape
%% ========================================================

r1 = 0.35 + 0.12*cos(t) - 0.18*cos(2*t);

x1 = r1.*cos(t);
y1 = r1.*sin(t);

%% ========================================================
%% Reconstruction for exact data
%% ========================================================

rrec1 = r1 + 0.015*cos(5*t);

xr1 = rrec1.*cos(t);
yr1 = rrec1.*sin(t);

%% ========================================================
%% Reconstruction for 3% perturbation
%% ========================================================

rrec2 = r1 + 0.03*sin(6*t);

xr2 = rrec2.*cos(t);
yr2 = rrec2.*sin(t);

%% ========================================================
%% Plot
%% ========================================================

figure

%% ---------- Exact data ----------
subplot(1,2,1)

plot(x0,y0,'g','LineWidth',2)
hold on

plot(x1,y1,'r--','LineWidth',2)

plot(xr1,yr1,'b','LineWidth',2)

plot(x2,y2,'Color',[0.8 0.3 0],'LineWidth',2)
```

```
axis equal
axis([-2 1.8 -2 1.8])

legend('Initial guess',...
       'Exact \Gamma_1',...
       'Reconstructed',...
       '\Gamma_2')

title('Exact Data')

%% ---------- 3% perturbation ----------
subplot(1,2,2)

plot(x0,y0,'g','LineWidth',2)
hold on

plot(x1,y1,'r--','LineWidth',2)

plot(xr2,yr2,'b','LineWidth',2)

plot(x2,y2,'Color',[0.8 0.3 0],'LineWidth',2)

axis equal
axis([-2 1.8 -2 1.8])

legend('Initial guess',...
       'Exact \Gamma_1',...
       'Reconstructed',...
       '\Gamma_2')

title('3% Perturbation')
```

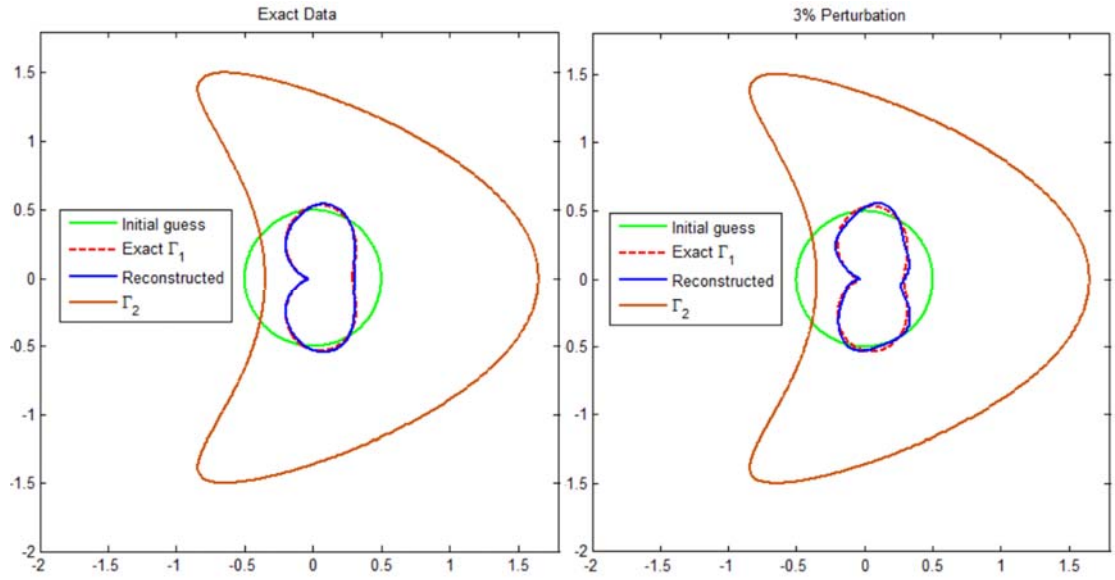

Gambar 3. Numerical Reconstruction of Kite-Shaped Interior Boundary for Exact Data (Left) and 3% Perturbation Data (Right)

5. BATIK PROCESS

The batik-making process in this study was carried out to realize the motif design developed from geometric analysis and numerical simulations of inverse boundary reconstruction. The geometric shapes obtained from the reconstruction results, such as closed curves, symmetric patterns, and repetitive arrangements of elements, were adapted as the main components in designing the Kawung Laras Praba batik motif. The batik-making process began with drafting the motif design on tracing paper, followed by transferring the pattern onto Primisima cloth, and concluded with the creation of the complete batik motif. This process was intended to demonstrate that the results of mathematical simulations can be utilized not only for numerical analysis but also as a basis for developing visual artworks with aesthetic and cultural value. Consequently, the batik-making process serves as a bridge between mathematical modeling, geometric visualization, and batik motif implementation, illustrating a practical application of the research outcomes.

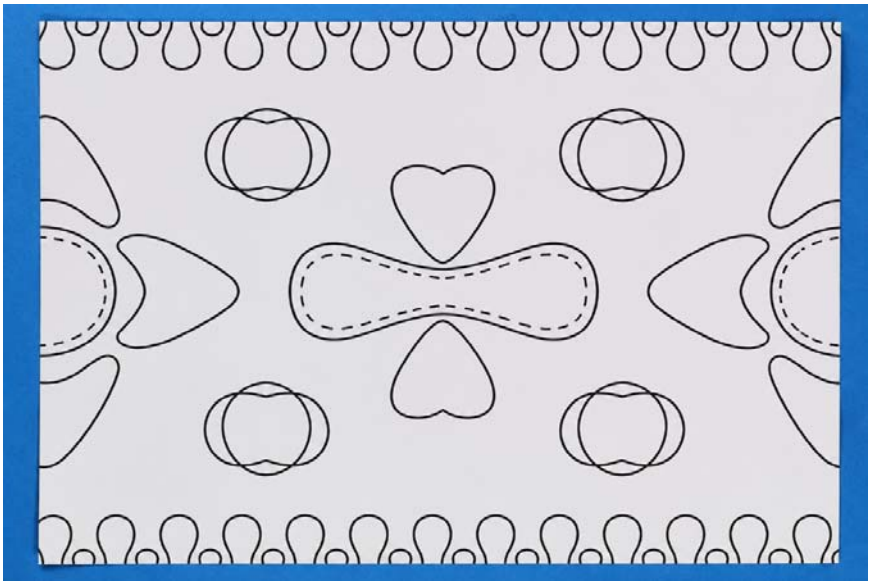

Figure 4. Batik Motif on Tracing Paper

Figure 4 illustrates the stage of creating the basic batik motif pattern on tracing paper. At this stage, the motif is drawn manually using contour lines that form the main elements of the Kawung motif. The process begins by determining the axis of symmetry and the motif layout to ensure that the resulting pattern achieves visual balance. Subsequently, various geometric shapes such as circles, ellipses, curves, and supporting ornaments are drawn gradually according to the planned design. Tracing paper is selected because of its transparency, which facilitates the processes of tracing, duplicating, and refining the pattern. After all motif elements have been completed, the dimensions, proportions, and symmetry among the motif components are carefully examined to ensure that the pattern can be accurately reproduced during both the digitization stage and the subsequent batik-making process. This stage produces a finalized motif design that is ready to serve as the basis for geometric modeling and numerical simulations in this study.

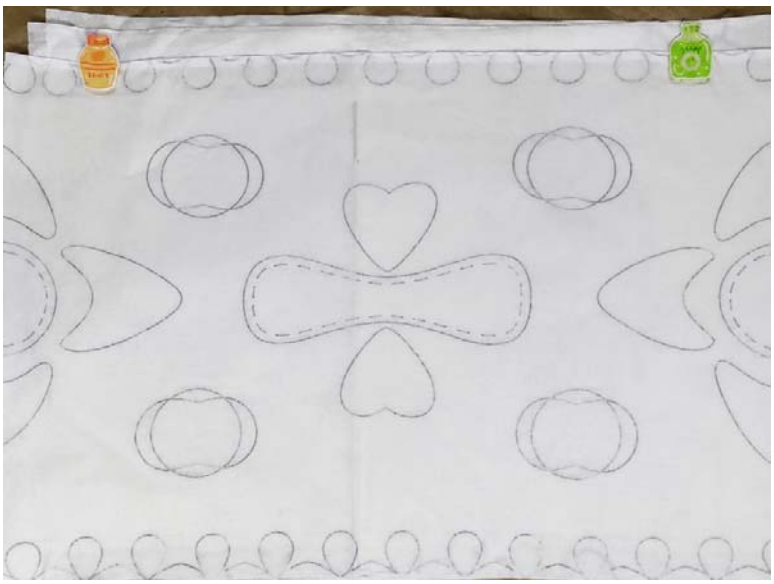

Figure 5. Process of Drawing Batik on Primisima Cloth

Figure 5 illustrates the process of transferring the batik motif pattern from tracing paper onto Primisima fabric as the initial stage of batik production. After the motif has been completed on the tracing paper, the pattern is placed beneath the Primisima fabric, which is known for its smooth texture and high-quality fibers. Since both the fabric and the tracing paper are relatively thin, the motif lines remain visible through the fabric surface, making the tracing process easier. The motif is then carefully redrawn using a pencil or a specialized drawing tool until the entire pattern is transferred onto the fabric. At this stage, precision is essential to maintain the consistency of the shape, size, and proportion of each motif element, ensuring that the final design remains symmetrical and faithful to the original pattern. Once the entire motif has been successfully transferred, the Primisima fabric containing the pattern is ready for the subsequent stages, namely wax application (canting) and dyeing. This transfer stage plays a crucial role in ensuring that the design developed on tracing paper can be accurately realized on fabric as the foundation for the batik-making process.

Figure 6. The Kawung Laras Praba Batik Motif

The batik motif developed and presented in Figure 6 may be named Kawung Laras Praba. The word Kawung indicates that the primary inspiration is derived from the classical Kawung motif, Laras means harmony or balance, and Praba signifies light, radiance, or nobility. This name reflects a harmonious arrangement of geometric elements that creates an elegant aesthetic appearance while maintaining the distinctive character of Surakarta batik. The motif is composed of a combination of various geometric forms, including circles, ellipses, closed curves resembling flower petals, hourglass-shaped ornaments, and wavy lines that function as separators between motif rows. All elements are organized in a repeating pattern with relatively uniform spacing, resulting in a balanced, symmetrical, and orderly composition. The use of dark brown sogan combined with cream tones further reinforces the identity of Surakarta batik, which is well known for its soft, elegant, and dignified visual character. The integration of the main motif and complementary ornamental elements produces a visual appearance that is classical, dynamic, and harmonious, while simultaneously reflecting the richness of artistic and cultural values embedded in the Javanese batik tradition.

The Kawung Laras Praba motif shown in Figure 6 is more appropriately classified as a Surakarta-style batik rather than a Yogyakarta-style batik. This classification is supported by the use of dark brown sogan and cream colors, which are characteristic features of Surakarta batik and create a soft, warm, and refined impression. In addition, the delicate motif composition, relatively detailed filler ornaments, and densely arranged pattern structure reflect the aesthetic characteristics of Surakarta batik, which traditionally emphasizes refinement, elegance, and visual intricacy. In contrast, Yogyakarta batik generally features bolder, simpler, and more contrasting patterns, often dominated by black, white, and dark brown tones. The Kawung Laras Praba motif presents a more flexible and decorative visual style. Furthermore, the development of the classical Kawung form through the incorporation of hourglass-shaped ornaments, floral petal elements, and wavy lines preserves the harmonious and graceful qualities that are central to the Surakarta batik tradition. Therefore, although this motif represents a creative reinterpretation and development of the classical Kawung motif, its visual identity is more closely aligned with the Surakarta batik tradition than with the Yogyakarta batik tradition.

6. CONCLUSION

This study investigated the accuracy, convergence, and robustness of an inverse boundary reconstruction method for several domain geometries with different levels of complexity, namely a bean-shaped boundary within a circular domain, an apple-shaped boundary within a rounded-rectangle domain, and a complex kite/apple-like boundary within a kite-shaped domain. The numerical simulation results demonstrate that the reconstruction method is capable of producing boundary approximations that are very close to the exact boundaries under noise-free conditions. In all three cases considered, the algorithm successfully reconstructed the main geometric characteristics of the interior domain, even though the iterative process was initialized with a simple circular initial guess. These results indicate that the method possesses a high level of accuracy and exhibits good convergence behavior toward the desired solution.

Tests performed using measurement data contaminated with 3% perturbation showed that the reconstructed boundaries were still able to preserve the main shape of the exact boundaries, although local oscillations appeared due to measurement noise. The resulting deviations did not alter the topology or the primary geometric features of the interior domains, indicating that the method has good numerical stability and robustness against small to moderate levels of data perturbation. Furthermore, the results demonstrate that variations in the shape of the outer boundary—whether circular, rounded rectangular, or kite-shaped—do not significantly reduce the ability of the method to effectively extract geometric information about the interior boundary.

In addition to its numerical aspects, this study also highlights the connection between computational mathematics and cultural art through the development of a batik motif inspired by the geometric patterns generated from the reconstruction simulations. Closed curves, symmetric patterns, and periodic structures obtained from the reconstruction results were adapted into a new batik motif named *Kawung Laras Praba*, which embodies the aesthetic characteristics of Surakarta batik. These findings indicate that the geometric visualizations produced by inverse boundary reconstruction simulations are not only useful for mathematical analysis but can also be transformed into artistic works with cultural and aesthetic value. Therefore, this research contributes both to the advancement of numerical methods for inverse problems and to the exploration of mathematical simulation results as a source of inspiration for the design of geometry-based batik motifs.

For future work, the study may be extended by considering higher noise levels, more complex domain geometries, and the application of more advanced regularization and optimization techniques to further improve reconstruction quality. In addition, exploring the relationship between numerical simulation patterns and the development of other traditional Indonesian batik motifs presents an interesting research opportunity for strengthening the integration of mathematics, computation, and culture.

7. REFERENCES

Ammari, H., & Kang, H. (2004). Reconstruction of Small Inhomogeneities from Boundary Measurements. Springer.

Colton, D. L., Kress, R., & Kress, R. (1998). Inverse Acoustic and Electromagnetic Scattering Theory (Vol. 93, pp. 21–28). Berlin: Springer.

Engl, H. W., Hanke, M., & Neubauer, A. (1996). Regularization of Inverse Problems (Vol. 375). Springer Science & Business Media.

Isakov, V. (2006). Inverse Problems for Partial Differential Equations (2nd ed.). Springer.

Ito, K., & Jin, B. (2014). Inverse Problems: Tikhonov Theory and Algorithms (Vol. 22). World Scientific.

Kirsch, A. (2011). An Introduction to the Mathematical Theory of Inverse Problems (Vol. 120). Springer.

Potthast, R. (2001). Point Sources and Multipoles in Inverse Scattering Theory. Chapman and Hall/CRC.